Effect of deformation temperature on microstructure evolution in aluminum alloy 2219 during hot ECAP

I. Mazurina , T. Sakai , H. Miura , O. Sitdikov , R. Kaibyshev

Abstract

The effect of deformation temperature on microstructure evolution during equal channel angular pressing (ECAP) was studied in a coarse-grained aluminum alloy 2219 in a wide temperature interval from 250 to 475 °C. The structural changes taking place during ECAP up to strains of 12 are classified into the following three stages irrespective of deformation temperatures: i.e. (1) an incubation period for formation of the embryos of deformation bands (DBs) at low strains; (2) development of large-scale DBs followed by grain fragmentation at moderate strains; (3) rapid development of new grain at high strains. Microstructure development in stages 1 and 2 is hardly influenced by temperature, while that in stage 3 is most significantly affected at higher temperature. An increase in the pressing temperature leads to decreasing the volume fraction of new grains and increasing the average grain size in stage 3. This can be attributed to relaxation of strain compatibility between grains due to frequent operation of dynamic recovery and grain boundary sliding at higher temperature. The mechanism of grain refinement is discussed in detail.

Keywords: Equal channel angular pressing (ECAP); Temperature effect; Deformation bands (DBs); Microstructure evolution; Grain refinement; Aluminum alloy

1. Introduction

Microstructural changes in aluminum (Al) and its alloys during equal channel angular pressing (ECAP) have been studied at various temperatures in previous papers (e.g. [1–11]). It was found that final grain size and the fraction of evolved low angle boundaries (LABs) are in general increased with increasing temperature of ECAP. The formation of new grains in Al-based alloys has been proposed as a result of the transformation of LABs formed at early stages of deformation into high angle boundaries (HABs) accompanied by dynamic recovery during hot deformation. This mechanism is similar to in situ or continuous dynamic recrystallization (cDRX) [1,4,7,8,12–15]. It is suggested in [1–8] that the transition of LABs into HABs can be controlled by a recovery rate, which is accelerated with increasing temperature. On the other hand, the fraction of HABs as well as the average misorientation angle increases faster in Al alloy at lower temperature [1,3–7,9–11]. The transformation of deformation-induced LABs into HABs hardly takes place at elevated temperatures, however, the new HABs start to form at a similar critical strain at various temperatures [7,12]. It was also pointed in [7] that the characteristics of new grain structure developed at high strains are almost similar irrespective of pressing temperature. On the other hand, the occurrence of cDRX during severe plastic deformation at high temperature has also been recognized as the geometric dynamic recrystallization (gDRX), which results in an equiaxed grain structure with a small grain size comparable to the subgrain size [8,16,17]. Serrated original grain boundaries impinge on each other during hot deformation and finally new fine grains are evolved in large strain without operation of any new recrystallization mechanism [17]. Thus, the effect on new grain formation in Al alloys and the mechanism operating during hot ECAP are still unclear in a wide range of temperatures.

The main aim of the present work was to study the effect of deformation temperature on microstructural changes as well as new grain formation taking place in Al alloy 2219 during hot ECAP. Special attention was paid to analyze the relationship between strain-induced grain structure and pressing temperature and the characteristics of strain-induced boundaries developed in a wide range of temperatures. The main factors promoting

grain refinement at various temperatures are analyzed and the mechanisms of new grain formation are discussed in details.

2. Experimental technique

An Al alloy 2219 with the following chemical composition (in mass%), such as 6.4Cu, 0.3Mn, 0.18Cr, 0.19Zr, 0.06Fe, was prepared by semicontinuous casting method at the Kaiser Aluminum Center for Technology. Homogenization was performed at 530 °C for 6 h with subsequent cooling in a furnace. The alloy had an equiaxed grain structure with an average size of about 140 μm. Samples were machined parallel to the ingot axis into rods with a diameter of 20 mm and a length of around 100 mm. ECAP was carried out at temperatures of 250, 300, 400 and 475 °C using a die with an L-shape configuration of circular channels. The details of processing are described elsewhere [4,14]. Each passage through the die resulted in a strain of about 1. The samples were repeatedly deformed up to strains of 12 at each temperature, using route A, i.e. without changing the orientation of samples with respect to the pressing direction (PD).

The ECAPed samples were cut from the center of each rod in longitudinal section parallel to the PD for microstructural observations. The metallographic analysis was carried out using an optical microscopy (OM) on the specimens etched by the standard dicks Keller's reagent. Specimens for electron backscattering diffraction pattern (EBSD) analysis were electropolished in a solution of 30% HNO_3 and 70% CH_3OH cooling by nitrogen to around −30 °C for the samples deformed at 250 and 300 °C, or in solution of 80% C_2H_5OH, 12% 2*n*-butoxyethanol, 8% $HClO_4$ at room temperature for the samples deformed at 400 and 475 °C. The orientation imaging microscopy (OIM) with automated indexing of electron back scattering diffraction (EBSD) patterns was performed in Hitachi S-4300H scanning electron microscope (SEM) with OIM analysis software provided by TexSem Lab Inc. The examining areas were automatically scanned with steps of 0.3, 0.4, 0.5 and 1.5 μm for the samples deformed at 250, 300, 400 and 475 °C, respectively. The misorientation distributions for strain induced (sub)grain boundaries were obtained from EBSD data in a whole scanned area and also in strain-induced fine-grained regions developed. The volume fraction of new fine grains V_{rex} surrounded by HABs with misorientations above 15° was calculated on the OIM maps using the conventional point counting technique. The average grain size achieved at high strains was measured by mean linear intercept method in the fine-grained regions developed. The average transverse size of (sub)grains and minimal width of DBs was measured perpendicular to the microstructure orientation direction.

3. Results

3.1. Microstructural evolution at various temperatures

Typical optical microstructures evolved during ECAP at strains of 3 and 12 at 300 and 475 °C are shown in Fig. 1. Fibrous microstructures consisting of numerous deformation bands (DBs) are aligned roughly parallel to pressing direction (PD) and developed heterogeneously in grain interiors at moderate strain of 3. With increasing temperature, well defined (sub)grain structures are developed inside the DBs. After ECAP

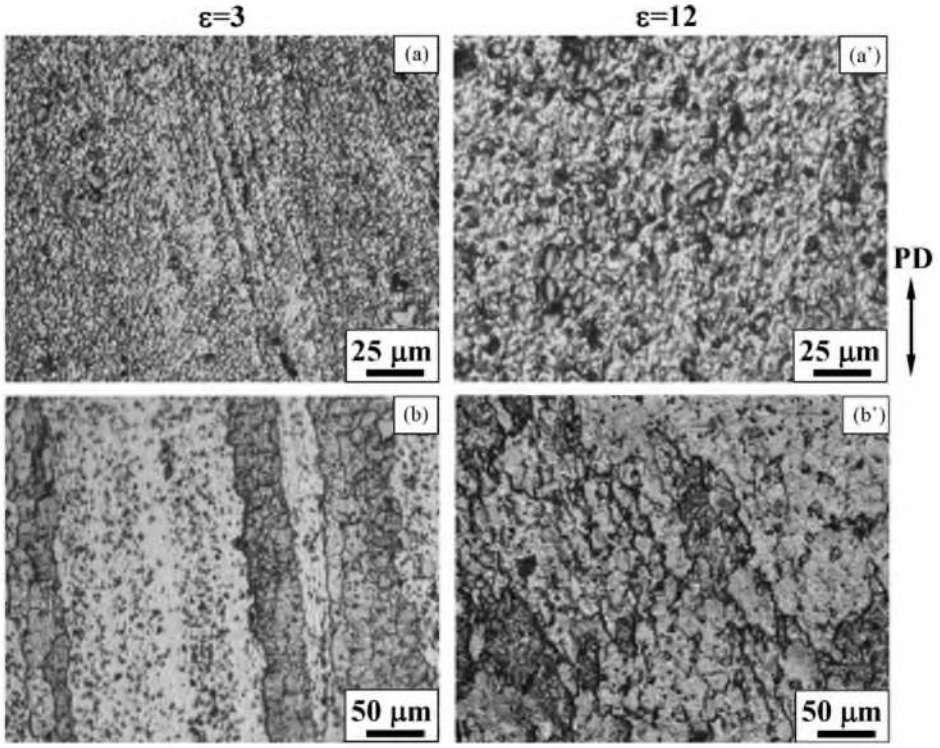

Fig. 1. Optical micrographs of 2219 Al alloy deformed by ECAP to strains of 3 and 12 at various temperatures: (a and a′) 300 °C; (b and b′) 475 °C; PD is the pressing direction.

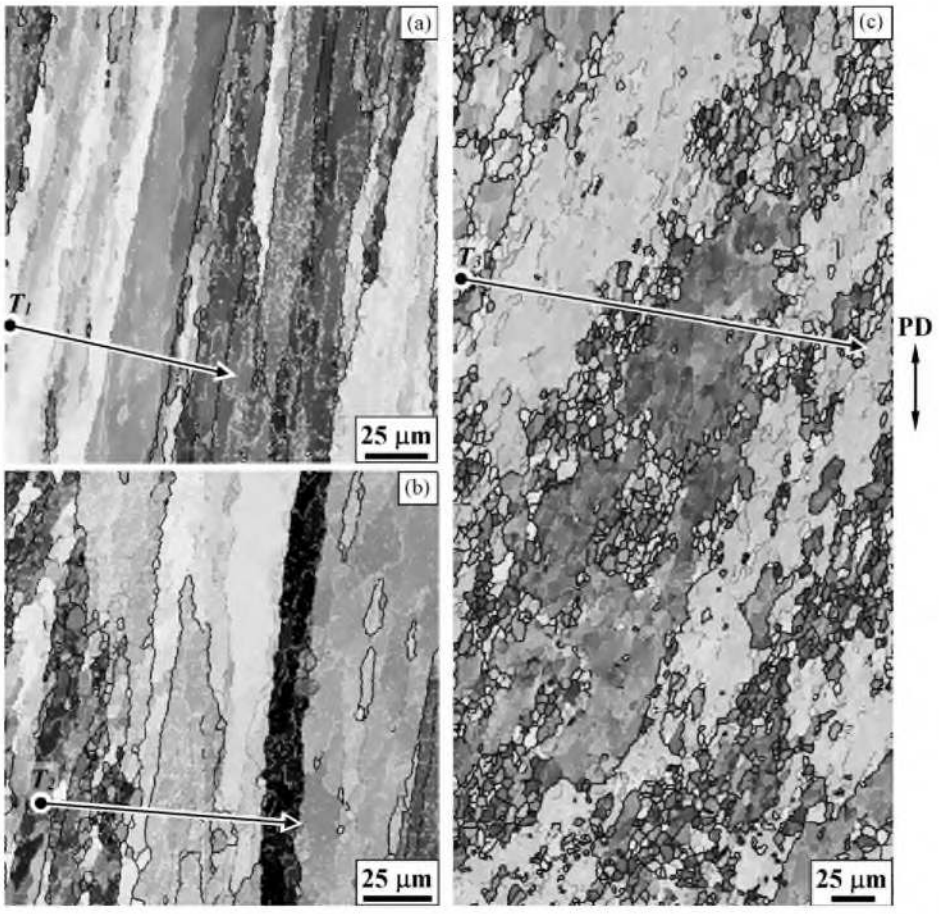

Fig. 2. Typical OIM micrographs of 2219 Al alloy deformed by ECAP at 400 °C. Thin white lines correspond to the boundaries with misorientation $\Theta > 2°$, thin black lines $\Theta > 5°$ and bold lines $\Theta \geq 15°$, respectively. (a) $\varepsilon = 2$; (b) $\varepsilon = 4$; (c) $\varepsilon = 8$.

to $\varepsilon = 12$, a very fine granular structure is homogeneously developed at 300 °C, but a rather coarser-grained structure is incompletely formed at 475 °C. The latter is a mixed structure composed of (sub)grains and coarser grains elongated to PD.

Let us examine in more detail the deformed microstructures developed during ECAP using SEM/EBSD. Typical OIM micrographs of the microstructures formed at 400 °C are shown in Fig. 2. In these maps, orientation difference ($\Delta\Theta$) between neighboring points, $\Theta \geq 2°$, $\Theta > 5°$, $\Theta \geq 15°$, are marked by white, thin black and bold black lines, respectively. At early stages of ECAP (e.g. $\varepsilon = 2$), initial coarse grains are subdivided by rather smooth dislocation boundaries with low-to-moderate angle misorientation, that are formed roughly parallel to PD, and also low angle dislocation boundaries are homogeneously developed in the grain interiors (Fig. 2(a)). With further deformation to $\varepsilon = 4$, well defined banded structures containing DBs and new fine (sub)grains are developed in colony along parts of the boundaries of DBs. In the other regions, DBs are scarcely formed and only subgrains with LABs are homogeneously developed. The regions of new fine grains are evolved with further deformation, while coarse grains containing mainly (sub)grains surrounded by LABs still exist stably in high strain interval (see Fig. 2(c) and also Fig. 5(c)).

Changes in the misorientation distributions, i.e. the point-to-point $\Delta\Theta$ and the point-to-origin $\sum\Delta\Theta$, were measured along test lines T_i indicated in Fig. 2. The results are represented in Fig. 3. The $\Delta\Theta$ developed at $\varepsilon = 2$ generally ranges from 2° to 5° and this may correspond to conventional (sub)grain boundaries. The $\Delta\Theta$ increases above 5–10° in several local places of grain interiors. These moderate misorientation angles belong to the boundaries of embryos of DBs [14]. The cumulative misorientation $\sum\Delta\Theta$ is alternated at such moderate boundaries of DBs. The $\Delta\Theta$ of above 30° at distance of around 60 μm in Fig. 3(a) may correspond to neighboring grain boundaries. After straining to $\varepsilon = 4$, moderate-to-high angle boundaries are frequently formed in the left hand side in Fig. 3(b), where new grains are developed in colony along the boundaries of large-scale DBs (Fig. 2(b)). The misorientation angles across the boundaries rapidly increase with straining, resulting in formation of new grains primarily along DBs. On the other hand, in the right hand side of Figs. 2(b) and 3(b), boundaries of conventional subgrains with LABs and some embryos of DBs with moderate angles are developed in coarse grain interiors. With deformation to $\varepsilon = 8$, two types of such microstructures, i.e. new fine grains with HABs evolved in colony and coarse grains containing substructure with LABs, are further developed alternatively, as can be seen in Figs. 2(c), 3(c) and 5(c). Here $\Delta\Theta$ measured along line T_3 in Fig. 2(c) ranges from 30° to 60° partly in the left, central and right hand side where fine grains are formed. In contrast, the $\Delta\Theta$ does not exceed 10° in intermediate areas

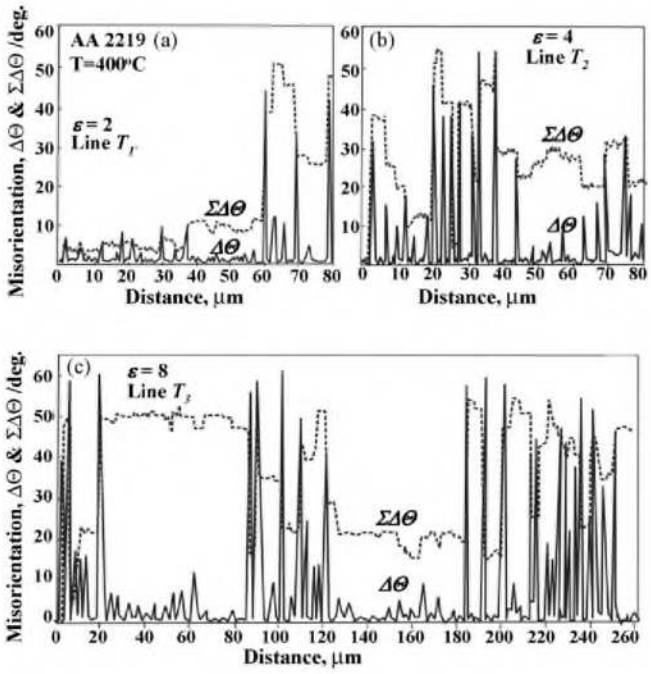

Fig. 3. Misorientation distribution of strain-induced boundaries in 2219 Al alloy developed along the lines (a) T_1, (b) T_2, and (c) T_3 indicated in Fig. 2(a–c), respectively.

where conventional substructure and some embryos of DBs are formed in original coarse grain interiors. Such inhomogeneous microstructures may be developed depending on whether DBs are easily or hardly formed in each original grain.

Fig. 4 represents changes in the average crystallite transverse sizes measured perpendicular to the microstructure orientation direction in the regions of strain-induced fine grains and in coarse grain interiors, as well as the minimal width of DBs,

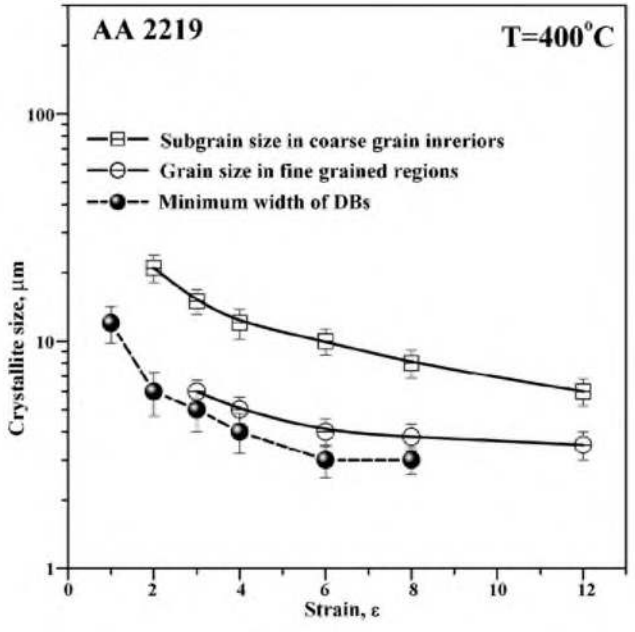

Fig. 4. Strain dependence of the average transverse crystallite size for 2219 Al alloy at 400 °C.

with repeated ECAP at 400 °C. It is interesting to note that all of the mentioned parameters rapidly decrease with straining to $\varepsilon = 6$ and approach constant values at high strains, and especially that the average grain size in the fine grain regions is almost similar to the width of DBs. The latter suggests that the strain-induced new grain development may be mainly controlled by a formation of large-scale DBs. In other words, the mechanism of grain refinement in the present Al alloy can be directly associated with grain fragmentation due to development of DBs.

The microstructures developed at a strain of 12 at various temperatures are represented in Fig. 5. It can be clearly seen that area of developed fine grains decreases with increasing of pressing temperature, and its average grain size increases. At lower temperatures of 250 and 300 °C, new fine grains with size of a micron are almost fully developed in a whole area. In contrast, colonies of strain-induced fine grains with HABs are mixed with rather coarse grains containing subgrains with LABs at higher temperatures of 400 and 475 °C. For example, comparing the microstructure that evolved at 400 °C at $\varepsilon = 8$ (Fig. 2(c)) to that at $\varepsilon = 12$ (Fig. 5(c)), the volume fraction of fine grains clearly increases with repeated ECAP, while the average grain size developed in colonies is almost similar. It should be noted that such strain-induced fine grains are evolved roughly parallel to the PD, suggesting that they may be formed along some large-scale DBs introduced by early ECAP (see Fig. 2). The microstructure evolved at 475 °C (Fig. 5(d)) shows almost similar features of that at 400 °C described above. It is noted in Fig. 5(d) that the average size of strain-induced new grains surrounded by HABs is smaller than that of (sub)grains formed in coarse grains (see also Fig. 4 for 400 °C).

3.2. Quantitative analysis of strain-induced grained structures

It is found in Section 3.1 that microstructures developed in the Al alloy 2219 during hot ECAP are sensitively affected by the pressing temperature. The deformed microstructures are categorized as the following two types, i.e. strain-induced fine grains surrounded by HABs that are evolved in colony and coarse grains containing subgrains with LABs, moreover the former fine-grained regions decrease with increasing deformation temperature. So these mixed microstructures should be analyzed separately in each of the regions. The misorientation distributions developed at strains of 3 and 12 are represented in Fig. 6. Here are the results measured in the regions of new grained structures as well as in a whole volume represented by broken and solid lines, respectively. The values of the average misorientation angle in each volume are also indicated by dashed and solid line arrows in Fig. 6.

Furthermore, changes of the misorientation distributions with ECAP at 250 °C are briefly reviewed here, because strain-induced fine grains are almost fully developed in high strain (see Fig. 5(a)). The main results are described elsewhere in [14]. The misorientation distributions with a single peak ranges mainly at lower angles below 5° at low strains below $\varepsilon = 2$. It starts to shift

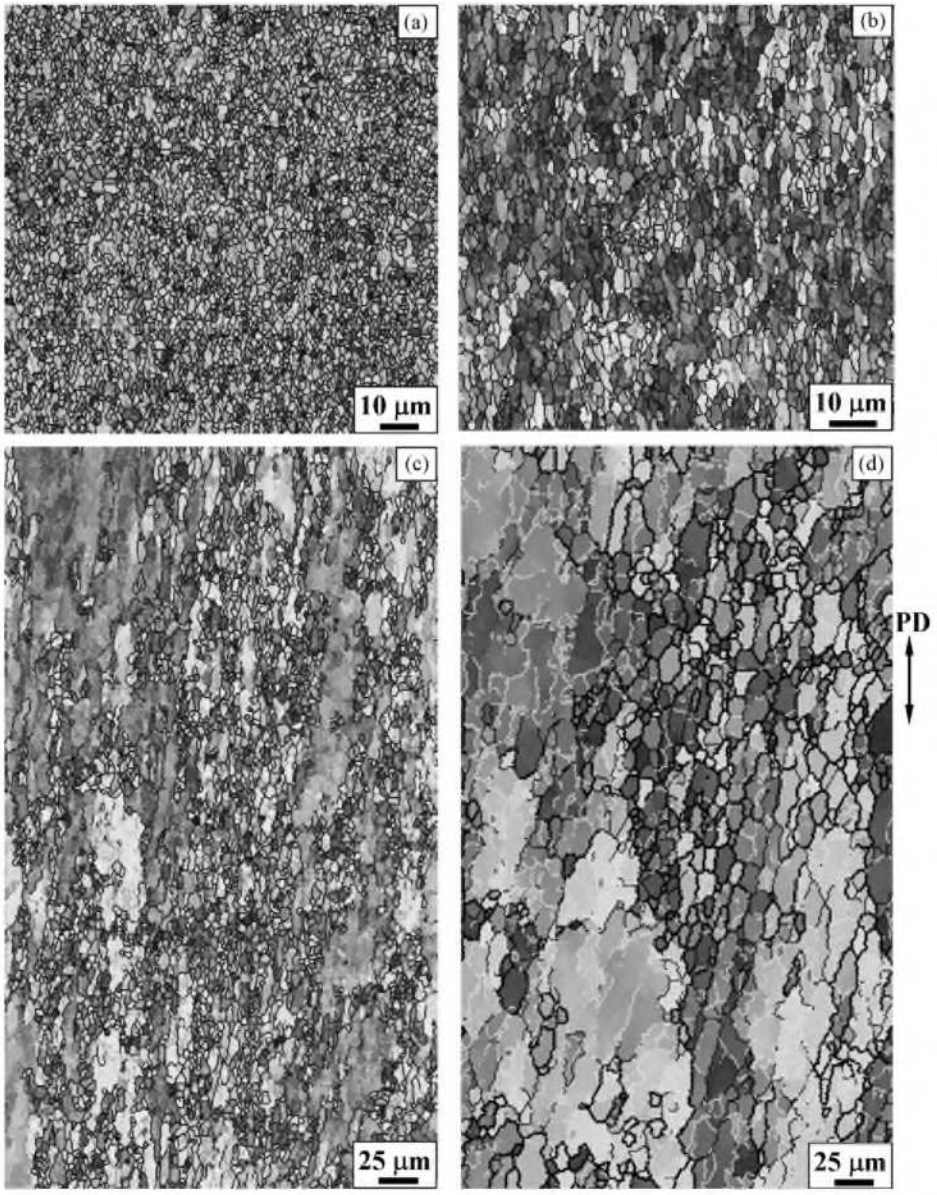

Fig. 5. OIM micrographs of 2219 Al alloy deformed by ECAP to a strain of 12 at various temperatures: (a) 250 °C; (b) 300 °C; (c) 400 °C; (d) 475 °C. PD is the pressing direction.

to higher misorientation angles accompanied by formation of DBs at strains above $\varepsilon = 3$. With further ECAP to higher strains, the fraction of LABs rapidly decreases and that of HABs contrary rises, resulting in a bimodal distribution with two peaks at around 5° and 50°. The distributions developed at $\varepsilon = 12$ are almost similar to a random one for annealed polycrystalline alloy [17].

Now let us analyze the present results obtained at higher temperatures (Fig. 6). The misorientation distributions developed at $\varepsilon < 3$ during early ECAP are not so much changed with increasing temperature from 300 to 475 °C. It is seen in Fig. 6(a–c) that the misorientations evolved at $\varepsilon = 3$ show a single peak type ranging mainly below 10°, while they shift a little to lower angles with increasing temperature (see the solid-line arrows). It is also noted here that the misoreintation distributions measured in a whole volume and in fine-grained regions are roughly similar at $\varepsilon < 3$. On the other hand, these misorientation distributions developed at $\varepsilon = 12$ shift to higher angles and show two peaks appearing at LABs and HABs, as shown in Fig. 6(d–f). The fraction of HABs with misorientations above 15° decreases and that of LABs conversely increases even with increase in temperature. It is remarkable to note that the misorientation distributions developed at $\varepsilon = 12$ in a whole volume (solid line) and in the fine-grained regions (dashed line) are clearly different at high temperatures of 400° and 475 °C, while those evolved at 300 °C are almost similar.

The average misorientation angle for strain-induced boundaries versus strain (Θ_{av}–ε) curves and temperature effect on them are represented in Fig. 7. The Θ_{av}–ε curves obtained in the whole volume and in the regions of strain-induced fine grains

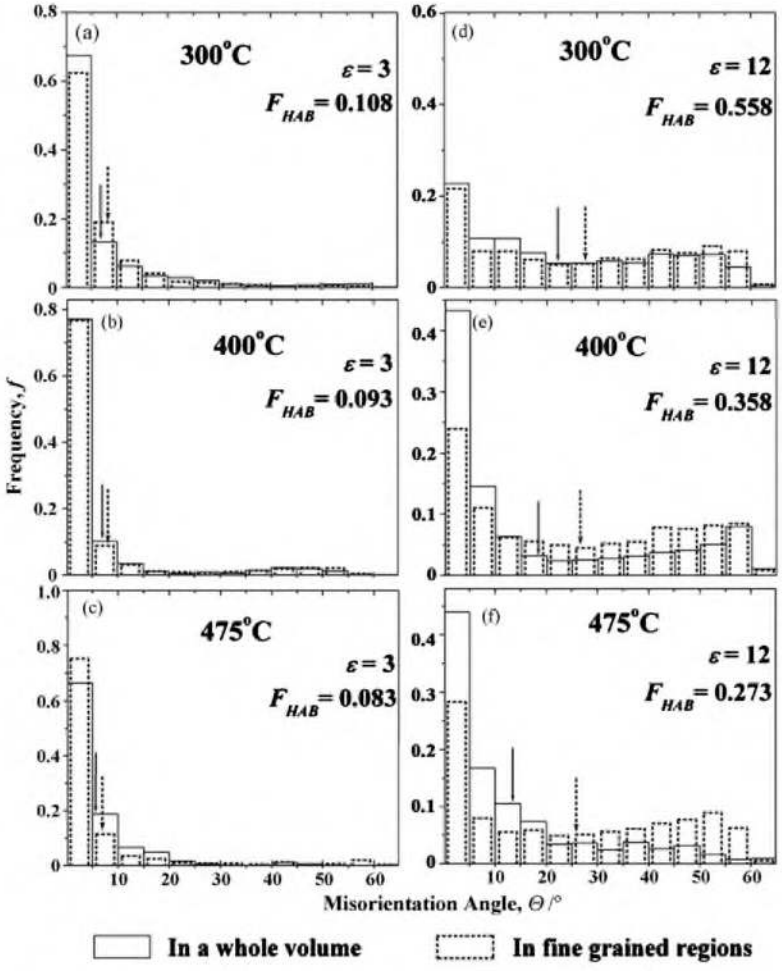

Fig. 6. Changes in the misorientation distribution of strain-induced boundaries developed in 2219 Al alloy deformed by ECAP to $\varepsilon = 3$ and $\varepsilon = 12$ at various temperatures. F_{HAB} and solid-line arrows indicate the fraction of HABs and the average misorientation angles measured in a whole volume. Broken line arrows show the Θ_{av} measured in fine-grained regions.

are depicted in Fig. 7(a and b), respectively. These Θ_{av}–ε curves can be classified into three stages irrespective of deformation temperature as follows:

(1) a rapid and limited increase of Θ_{av} leading to a plateau of about 3–5° in low strain ($\varepsilon < 2$);
(2) a steep increase of Θ_{av} occurring at a critical strain of around 2 in a moderate strain interval ($2 < \varepsilon < 4$);
(3) a gradual increase to a higher saturation value of Θ_{av} at high strain, which depends on temperature ($\varepsilon > 4$).

In stage 1, dislocation substructures with LABs developed at $\varepsilon \leq 2$ can result in a plateau of Θ_{av} 3–5°. In subsequent stage 2, moderate-to-high angle boundaries evolved in strain interval of 2–4 can be explained by the formation of embryos of DBs and their transformation into large-scale DBs (Figs. 1 and 2). In stage 3 appearing in high strain, the Θ_{av}–ε curves derived from a whole volume are clearly changed with increasing temperature (Fig. 7(a)), while that for fine-grained regions are not so much influenced by temperature (Fig. 7(b)). If the latter Θ_{av}–ε curves are assumed to be roughly similar within the experimental scatters, temperature dependence of the Θ_{av}–ε curves for a whole volume may be resulted mainly from an increase of the regions composed of remnant original coarse grains, where DBs are scarcely formed and dislocation subboundaries with LABs are developed (Figs. 2 and 5). The results of Fig. 7 may be very important for consideration of temperature effect on the formation of strain-induced fine grains during hot ECAP and so will be discussed in more detail in next section.

Finally, Fig. 8 shows temperature dependence of the average misorientation angle Θ_{av} in a whole volume and that in the fine-grained regions as well as the average size of new fine grains evolved at $\varepsilon = 12$. It can be seen in Fig. 8 that the Θ_{av} in a whole volume decreases rapidly with increasing temperature, while that in fine-grained regions changes scarcely at higher temperatures. The average size of strain-induced grains is around 1.5 μm at temperatures below 300 °C and starts to increase clearly at temperature of above 400 °C. It is interesting to note in Fig. 8 that the misorientation parameter of strain-induced grain boundaries in fine-grained regions does not change so much at high temperatures, while the average grain size increases with increasing temperature.

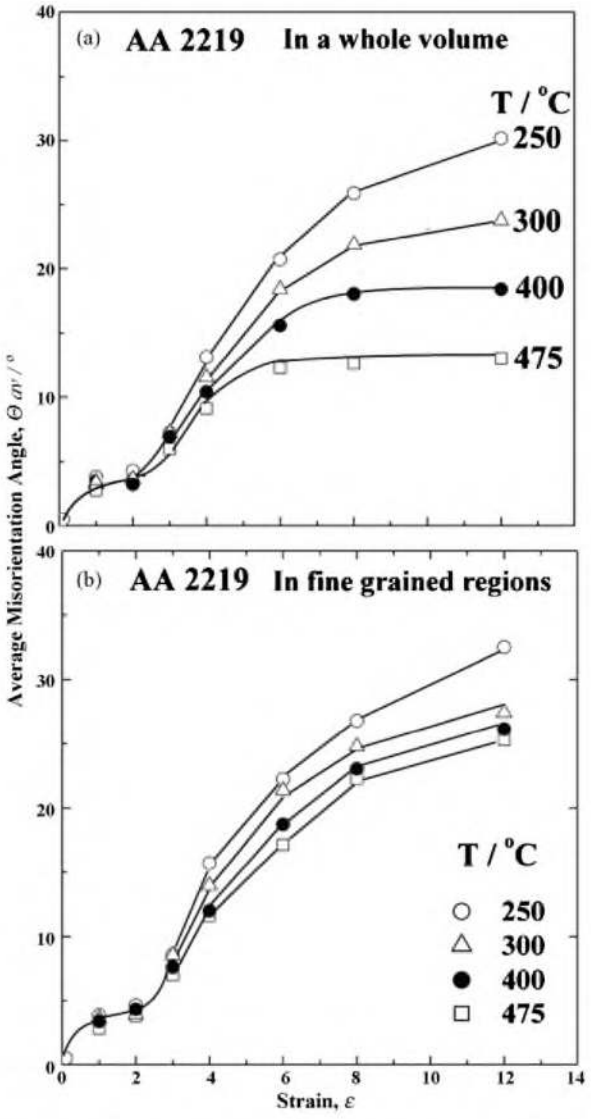

Fig. 7. Changes in average misorientation angle of strain-induced boundaries developed in 2219 Al alloy with repeated ECAP at various temperatures (a) in a whole volume and (b) in regions consisting of new fine grains only.

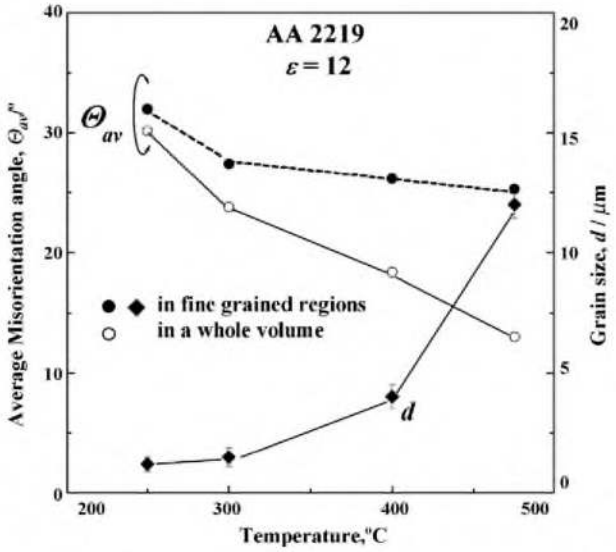

Fig. 8. Temperature dependence of average misorientation angle of strain-induced boundaries and new grain size developed in 2219 Al alloy at $\varepsilon = 12$.

4. Discussion

4.1. Strain-induced grain formation process

The process of strain-induced (sub)grain boundaries formation was studied in the Al alloy 2219 during ECAP at elevated temperatures. The results at 250 °C, described in detail elsewhere [14], are briefly summarized here. The processes follow three stages, as confirmed in Fig. 7. In stage 1 ($\varepsilon < 2$), conventional dislocation substructures with LABs are homogeneously developed accompanied with embryos of DBs, that is an incubation stage for formation of DBs. In stage 2 appearing at moderate strains ($\varepsilon = 2$–4), such embryos transform into large-scale DBs and their boundaries show moderate-to-high misorientation angles, leading to grain fragmentation into misoriented regions developed in original grain interiors. With further straining to above 4, i.e. in stage 3, new grains surrounded by HABs are developed in a whole material accompanied by randomization of the crystal orientation.

Such three stages of microstructural changes during hot ECAP do not change with deformation temperature (Fig. 7). It is clearly seen in Fig. 7 that temperature effect on microstructural evolution appears differently in each stage. Namely, in early two stages, i.e. at low to moderate strain, development of strain-induced subboundaries accompanied with embryos of DBs is scarcely affected by deformation temperature. This suggests that these processes may be considered as mechanically induced events and so a thermal ones [18]. It is shown in [17,19,20] that various kinds of DBs are developed in metallic materials during plastic deformation. They may be roughly categorized the DBs with transition boundaries having persistent nature, e.g. such as microshear bands and kink bands, and other various DBs with rather diffusive boundaries having temporary nature. The former DBs with persistent nature can be resulted from compatibility requirements of neighboring coarse grains or any intrinsic structural instability during large deformation [17–21]. Thus, microstructural developments in stages 1 and 2 are scarcely influenced by pressing temperature.

On the other hand, dynamic recovery can assist the transformation of strain-induced non-equilibrium boundaries to equilibrium ones and so the formation of new grains during large strain deformation at elevated temperatures [16,21]. Repeated large strain deformation can give enough time for dislocation rearrangement taking place in various strain-induced boundaries, leading to both increase of grain boundary misorientation and decrease of dislocation density in subgrain interiors [22]. It may be concluded, therefore, that strain-induced grain formation results from dynamic formation of HABs in stages 1 and 2, followed by frequent operation of dynamic recovery in the HABs at large strains, i.e. in stage 3. The latter may be connected with the fact that the average misorientation angle versus strain (Θ_{av}–ε) curve is changed sensitively with deformation temperature at high strains above 4. Microstructure changes in stage 3 are con-

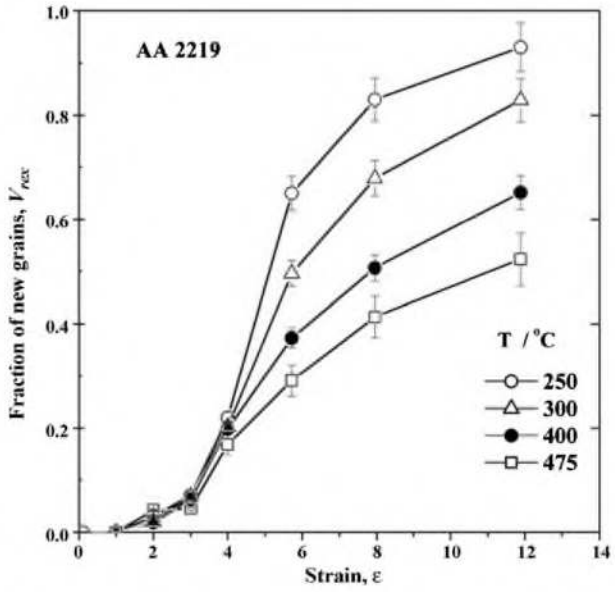

Fig. 9. Strain dependence of volume fraction of new fine grains V_{rex} developed in 2219 Al alloy during ECAP at various temperatures.

sidered, therefore, to be controlled by athermally activated rate process [18]. Let us discuss the temperature effect on new grain formation during ECAP in more detail in next section.

4.2. *Temperature effect on new grain formation*

All the present results in Figs. 1–8 allow us to consider an important role of deformation temperature on strain-induced grain formation that appears remarkably in high strain, i.e. in stage 3, under ECAP conditions. It is noted in Fig. 7 that the Θ_{av}–ε curves plotted for a whole volume are changed sensitively depending on deformation temperature, while those in fine-grained regions shows relatively smaller temperature dependence. The data in the latter case may be considered as roughly similar irrespective pressing temperature within some experimental scatters. This suggests that the structure characteristics in fine-grained regions are hardly affected by deformation temperature. On the other hand, the volume fraction of the new grain structure should be largely decreased with increasing temperature, as can be seen in Figs. 1, 2 and 5.

The volume fraction of fine grains V_{rex} surrounded by HABs with misorientations above 15° was measured using OIM maps. The V_{rex}–ε curves at various temperatures are depicted in Fig. 9. The shape of these curves looks similar to that of the Θ_{av}–ε ones in Fig. 7(a); namely V_{rex} is roughly zero at $\varepsilon < 2$ (stage 1), then it starts to increase rapidly at $2 < \varepsilon < 4$ (stage 2) and finally gradually increases at $\varepsilon > 4$ (stage 3). Temperature effect on the V_{rex}–ε curves also looks similar to that on the Θ_{av}–ε ones in a whole volume and appears remarkably in stage 3. It may be concluded from Figs. 7(a) and 9, therefore, that the temperature effect on the Θ_{av} in a whole volume can be controlled mainly by that on the V_{rex}. Let us discuss how deformation temperature can affect the development of strain-induced new grains at high strains.

During large strain deformation at elevated temperatures, the deformation becomes more homogeneous because of frequent operation of dynamic recovery, as discussed in Section 4.1. Grain boundary sliding also operates especially in fine-grained regions developed by large strain deformation [7,12,13,21]. Under such conditions, DBs can be hardly developed in remained coarse grain interiors at elevated temperatures through relaxation of strain heterogeneity resulted from compatibility requirements of neighboring grains or any intrinsic instability of remained grain interiors [14,15]. Ball and Humphreys [23] and Duckhan at al. [24] observed temperature effect on the formation of large-scale DBs in Al alloys and showed that the tendency for shear banding becomes less common at elevated temperatures. The volume fraction of initial grains containing large-scale DBs decreases with increasing temperature and may be almost zero at high temperature above 400 °C [23,24].

On the other hand, the as-deformed samples should be usually exposured in ECAP channel die keeping at elevated temperatures and may be statically annealed during repeated ECAP processes. Sitdikov et al. observed bimodal grain structures developed in Al–6%Mg 0.3%Sc alloy during ECAP at 300 °C [15]. They concluded that two structural components can be resulted from simultaneous operation of cDRX, occurring during deformation, and static recrystallization during each ECAP pass. To study any effect of static annealing on the strain-induced grain structures, developed in the present alloy during ECAP, the samples deformed to $\varepsilon = 8$ at 400 °C were subsequently statically annealed at 400 °C for 50 min. The microstructural characteristics of fine grains in colony in the as-deformed and its annealed structures are summarized in Table 1. It is seen in Table 1 that static recrystallization does not take place, but static recovery operates during annealing leading to a small increase in V_{rex}, Θ_{av} and d mainly through disappearance of LABs. The present Al alloy contains high density of secondary precipitates of the θ-phase and some dispersoids of transition metals, such as Al_3Cr, Al_3Zr, Al_6Mn [4]. They may play an important role for retardation of dislocation rearrangements and stabilization of strain induced new grain structures during repeated ECAP.

Finally, let us consider a relationship between the fraction of HABs, F_{HAB} in fine-grained regions and the volume fraction of new grains, V_{rex}, at elevated temperatures, as represented in Fig. 10. It is noted in Fig. 10 that V_{rex} can be represented by a unique function of the F_{HAB} irrespective of strain and deformation temperature within the experimental scatters, and that the V_{rex} is smaller than the F_{HAB} in early ECAP, but

Table 1
Characteristics of strain-induced fine grains developed at $\varepsilon = 8$ during ECAP at 400° and subsequently annealed ones for 50 min

	V_{rex}[a]	Θ_{av}[a] (°)	d[a] (μm)
As-deformed	0.48	23.0	5–5.5
After annealing	0.49	23.5	6

[a] V_{rex}, Θ_{av} and d are the volume fraction, average misorientation angle and average grain size measured in fine-grained regions.

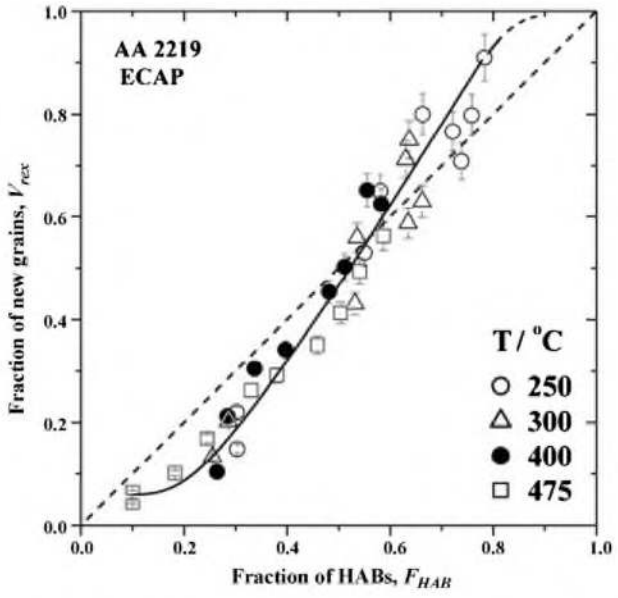

Fig. 10. Relationship between volume fractions of new fine grains V_{rex} and high angle boundaries F_{HAB} developed in 2219 Al alloy during ECAP.

conversely, larger in later stage at high strains. During early ECAP, HABs are introduced by formation of DBs and lead to grain fragmentation at low to moderate strain, and then followed by new grain formation. This is the reason why V_{rex} is smaller than F_{HAB} in early ECAP. With further repeated ECAP, V_{rex} rapidly increases and approaches F_{HAB} of around 0.5. The strain at which the V_{rex} attains 0.5 changes significantly with increasing temperature from $\varepsilon = 5$ at 250 °C to $\varepsilon = 12$ at 475 °C in Fig. 10. In later stages of ECAP, elongated as well as equiaxed new grains are homogeneously and fully developed in a whole area at 250 °C or 300 °C (Fig. 5(a or b)), where some fraction of LABs is always formed in a strain-induced structure (see Fig. 6). This is a typical characteristic of strain-induced grain structure [17] and that is why the fraction of HABs is smaller than V_{rex} or does not approach 100% at large strains.

5. Conclusions

The effect of deformation temperature on microstructure evolution in a coarse-grained 2219 Al alloy during ECAP to strains of 12 at various temperatures from 250 to 475 °C was studied in the present work. The main results are summarized as follows:

(1) The process of new fine grain formation during ECAP in a wide temperature interval can be classified into the three stages: (1) formation of conventional dislocation substructures accompanied with embryos of DBs in stage 1 ($\varepsilon < 2$); (2) development of large-scale DBs followed by grain fragmentation, leading to new grain formation along DBs at moderate strains in stage 2 ($2 < \varepsilon < 4$); (3) development of new grained structures at high strains in stage 3 ($\varepsilon > 4$).

(2) The deformed microstructures developed during ECAP at various temperatures are mixed ones and categorized into two types, i.e. strain-induced fine grains with HABs and coarse grains containing subgrains with LABs. The misorientation microstructure characteristics in fine-grained regions are hardly affected by deformation temperature, but the volume fraction of the new grains is largely decreased with increase in temperature due to less frequent formation of large-scale DBs.

(3) Microstructural development in a whole volume of the ECAPed Al alloy is hardly influenced by the pressing temperature in stages (1) and (2), while the formation of the new fine-grained structure is significantly affected by temperature at higher strains in stage (3). It is concluded that strain-induced grain formation results from dynamic formation of HABs in stages (1) and (2), followed by frequent operation of dynamic recovery in the HABs developed in stage (3).

Acknowledgments

The authors acknowledge with gratitude the financial supports received from Ministry of Education, Science and Culture (Grant-in-Aid for Scientific Research on Priority Area 457) and The Light Metals Education Foundation in Japan. One of the authors (I.M.) would like to express hearty thanks to the Japanese government for providing the scholarship.

References

[1] R.Z. Valiev, R.K. Islamgaliev, I.V. Alexandrov, Progr. Mater. Sci. 45 (2000) 103–189.
[2] A. Yamashita, D. Yamaguchi, Z. Horita, T.G. Langdon, Mater. Sci. Eng. A287 (2000) 100–106.
[3] J.Y. Chang, J.S. Yoon, G.H. Kim, Scripta Mater. 45 (2001) 347–354.
[4] O. Sitdikov, R. Kaibyshev, I. Safarov, I. Mazurina, Phys. Met. Metallogr. 92 (2001) 270–280.
[5] Y.C. Chen, Y.Y. Huang, C.P. Chang, P.W. Kao, Acta Mater. 51 (2003) 2005–2015.
[6] O.V. Mishin, D.J. Jensen, N. Hansen, Mater. Sci. Eng. A342 (2003) 320–328.
[7] A. Goloborodko, O. Sitdikov, R. Kaibyshev, H. Miura, T. Sakai, Mater. Sci. Eng. A381 (2004) 121–128.
[8] H.J. McQueen, Mat. Sci. Eng. A387–389 (2004) 203–208.
[9] P.J. Apps, M. Berta, P.B. Prangnell, Acta Mater. 53 (2005) 499–511.
[10] R.Z. Valiev, T.G. Langdon, Progr. Mater. Sci. 51 (2006) 881–981.
[11] A.P. Zhilyaev, D.L. Swisher, K. Oh-ishi, T.G. Langdon, T.R. McNelley, Mater. Sci. Eng. A429 (2006) 137–148.
[12] T. Sakai, in: Y.T. Zhu, T.G. Langdon, Z. Horita, M.J. Zehetbauer, S.L. Semiatin, T.C. Lowe (Eds.), Ultrafine Grained Materials IV, vol. 237, TMS, 2006, p. 73.
[13] O. Sitdikov, T. Sakai, E. Avtokratova, R. Kaibyshev, Y. Kimura, K. Tsuzaki, Mater. Sci. Eng. A444 (2007) 18–30.
[14] I. Mazurina, T. Sakai, H. Miura, O. Sitdikov, R. Kaibyshev, Mater. Sci. Eng. A (2007), doi:10.1016/j.msea.2007.04.112.
[15] O. Sitdikov, T. Sakai, E. Avtokratova, R. Kaibyshev, K. Tsuzaki, Y. Watanabe, Mater. Sci. Forum 558–559 (2007) 569–574.
[16] S. Gourdet, F. Montheillet, Mater. Sci. Eng. A283 (2000) 274–288.
[17] F.J. Humphreys, M. Hatherly, Recrystallization and Related Annealing Phenomena, second ed., Elsevier, 2004.
[18] C. Kobayashi, T. Sakai, A. Belyakov, H. Miura, Philos. Mag. Lett. 87 (2007) 751–766.

[19] D. Kuhlman-Wilsdorf, Metall. Mater. Trans. A35 (2004) 388–418.
[20] W.B. Hutchinson, Mater. Sci. Forum 558–559 (2007) 13–22.
[21] O. Sitdikov, T. Sakai, A. Goloborodko, H. Miura, R. Kaibyshev, Philos. Mag. 85 (2005) 1159–1175.
[22] A. Belyakov, T. Sakai, H. Miura, K. Tsuzaki, Philos. Mag. 81 (2001) 2629–2643.
[23] E. Ball, F.J. Humphreys, in: W.B. Hutchinson, et al. (Eds.), Thermomechanical Processing (TMP^2), ASM, Ohio, 1996, p. 184.
[24] A. Duckham, R.D. Knutsen, O. Engler, Acta Mater. 49 (2001) 2739–2749.